Substituent Effects in [2σ + 2σ + 2σ] Thermal Decarbonylation of Cage Ketones. Remarkably Effective Elongation of Strained C–C Bond by Through-Bond Coupling

Kazunobu Harano,[1a] Takashi Ban,[1a] Masami Yasuda,[1a] Eiji Ōsawa,[1b] and Ken Kanematsu*[1a]

Contribution from the Institute of Synthetic Organic Chemistry, Faculty of Pharmaceutical Sciences, Kyushu University, Fukuoka 812, and the Department of Chemistry, Faculty of Sciences, Hokkaido University, Sapporo 060, Japan. *Received July 28, 1980*

Abstract: Strained pentacyclic ketones (**5a–d**) were prepared in high yields by photoinduced [4 + 2]π cycloadduct of *N*-(ethoxycarbonyl)azepine with substituted cyclopentadienones. The structure of one of the cage ketones (**5d**) was confirmed by X-ray analysis to be 1,2-diphenyl-5,7-bis(methoxycarbonyl)-11-(ethoxycarbonyl)-11-azapentacyclo[5.5.0.0^{2,5}.0^{3,12}.0^{4,8}]-dodeca-9-en-6-one. The C_1(Ph)–C_2(Ph) bond of this molecule is extraordinarily long (1.657 (5) Å). Neither mechanical strain nor conventional through-bond interaction of phenyl π systems was satisfactory to interpret this elongation. We propose that the heightened σ level and lower σ* level of the prestrained C_1–C_2 bond, originally caused by the deformed carbon skeleton of **5**, lead to efficient mixing with the phenyl π orbitals. The enhanced "through-bond" interactions involving strained σ bond were demonstrated with combined molecular mechanics and MNDO calculations of model structures including 1,4-diphenylbicyclo[2.2.0]hexane. Also unusual in the observed structure of **5d** is the conformation of methoxycarbonyl groups adjacent to keto group, wherein three carbonyl dipoles align in nearly syn-parallel fashion. Compounds **5a–d** decarbonylate rapidly at 180 °C to give tricyclic trienes **6a–d** in quantitative yields. The thermally labile, long C_1–C_2 bond of **5** is suggested to play a key role in the ring opening. Decarbonylation rate increased 100-fold by changing the methyl group adjacent to carbonyl of **5a** to alkoxycarbonyls (**5d,e**). This rate enhancement was explained in terms of frontier orbital and steric theories.

In their pioneering work on the utilization of solar energy through valence isomerization between the tricyclic diene **2** (Ar = *p*-tolyl; R = CH_3; X = $(CH_2)_n$, n = 1–3) and the strained-cage molecule **3**, Mukai and his co-workers[2] prepared **2** by novel thermal decarbonylation of pentacyclic ketone **1** (Scheme I).

They recorded two remarkable features of the decarbonylation reaction: (1) one of the broken σ bonds must be doubly substituted with Ar groups and (2) the reaction proceeds smoothly when X is a three-carbon bridge. The role of Ar group appeared to stabilize the biradical transition state and the longer X bridge to induce higher strain in the C(Ar)–C(Ar) bond.[2] However, both molecular mechanics[3] and MINDO/3[2a] calculations agree in that the effect of inserting a three-carbon bridge upon the strain of the C_1–C_2 bond of unsubstituted **1** (Ar = H) as a model is minimal.

In the course of our studies on the synthetic design by logical assembling of molecules in the frontier-orbital-controlled pericyclic reactions of heteropines,[4a] we prepared a series of pentacyclic ketones **5a–e** related to **1**. They also undergo rapid decarbonylation to afford **6**. X-ray analysis revealed an unusually long bond in one of the ketones. This observation led to the recognition of a general bond-lengthening effect by the "through-bond" mechanism in strained C(Ph)–C(Ph) systems related to **5**.

Scheme I

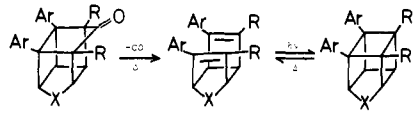

1 **2** **3**

Scheme II

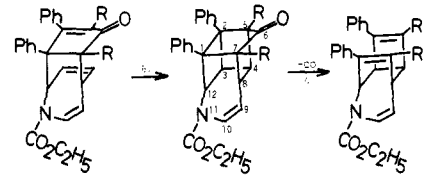

4a–e **5a–e** **6a–e**

a, R = CH_3; b, R = CH_2CH_3; c, R = $CH_2CH_2CH_3$; d, R = CO_2CH_3; e, R = $CO_2CH_2CH_3$

Results

Synthesis of Strained Pentacyclic Ketones. Irradiation of benzene solutions of the anti-endo [2 + 4]π cycloadducts (**4a–e**), which were obtained from 2,5-disubstituted-3,4-diphenyl-cyclopentadienones and (*N*-ethoxycarbonyl)azepine,[4a] gave pentacyclic ketones (**5a–e**) in high yields (Scheme II).

The results of photochemical synthesis of **5** are summarized in Table I and the NMR spectra of **5** in Tables II and III.

Table I. Photolyses of Anti-Endo [4 + 2] π Cycloadducts

compd	R	mp, °C	yield, %	IR ν(C=O), cm^{-1}		UV[a]	
				$CHCl_3$	Nujol	λ_{max}, nm	ϵ_{max}
5a	Me	209–210	98	1702 1758	1700 1753	255 (sh)	4300
5b	Et	171–172	96	1700 1752	1703 1750	256 (sh)	4400
5c	Pr	175–177	96	1702 1752	1703 1750	256 (sh)	4600
5d	CO_2Me	218–219	98	1708 1740 1788	1700 1730 1799	256 (sh)	5200
5e	CO_2Et	206–209	97	1712 1740 1788	1700 1730 1799	258 (sh)	5500

[a] Ethanol.

The four saturated and two olefinic protons in the azepine fragment of **5** appear well resolved, and their coupling constants were determined by the double-resonance technique. The keto groups of **5d** and **5e** are more congested than those of **5a–c**; the

(1) (a) Kyushu University. (b) Hokkaido University.
(2) (a) Mukai, T.; Yamashita, Y. *Tetrahedron Lett.* **1978**, 357. (b) Tezuka, T.; Yamashita, Y.; Mukai, T. *J. Am. Chem. Soc.* **1976**, *98*, 6051.
(3) Ōsawa, E.; Aigami, K.; Inamoto, Y. *J. Chem. Soc., Perkin Trans. 2* **1979**, 181.
(4) (a) Harano, K.; Yasuda, M.; Ban, T.; Kanematsu, K. *J. Org. Chem.* **1980**, *45*, 4455. (b) Mori, M; Hayamizu, A.; Kanematsu, K. *J. Chem. Soc., Perkin Trans. 1*, in the press.

0002-7863/81/1503-2310$01.25/0

Table II. ^{1}H NMR[a] Spectra of Cage Ketones

compd	chem shift, δ (J, Hz)
5a	1.08, 1.14 (s, $2CH_3$, 6 H), 1.32 (t, CH_3, 3 H), 2.20 (dd, H_8, 1 H, J = 8.0, 4.4), 3.14 (dd, H_4, 1 H, J = 7.6), 4.19 (dd, H_3, 1 H, J = 5.2), 4.23 (q, CH_2, 2 H), 4.72 (d, H_9, 1 H, J = 7.6), 5.54 (bs, H_{12}, 1 H), 6.78 (dd, H_{10}, 1 H), 6.92–7.06 (m, Ph-H, 10 H)
5b	0.72–0.96 (m, $2CH_3$, 6 H), 1.25–1.88 (m, $2CH_2$, 4 H), 1.32 (t, CH_3, 3 H), 2.38 (dd, H_8, 1 H, J = 4.8, 8.8), 3.37 (dd, H_4, 1 H, J = 7.0), 4.06 (dd, H_3, 1 H, J = 6.0), 4.25 (q, CH_2, 2 H), 4.80 (t, H_9, 1 H, J = 9.2), 5.52 (bs, H_{12}, 1 H), 6.80 (m, H_{10}, 1 H), 6.92 –7.08 (m, Ph-H, 10 H)
5c	0.81 (m, $2CH_3$, 6 H), 1.00–1.70 (m, $4CH_2$, 8 H), 1.34 (t, CH_3, 3 H), 2.37 (dd, H_8, 1 H, J = 4.8, 8.8), 3.36 (dd, H_4, 1 H, J = 6.9), 4.07 (dd, H_3, 1 H, J = 5.2), 4.25 (q, CH_2, 2 H), 4.78 (t, H_9, 1 H, J = 9.2), 5.52 (bs, H_{12}, 1 H), 6.80 (m, H_{10}, 1 H), 6.92–7.10 (m, Ph-H, 10 H)
5d	1.32 (t, CH_3, 3 H), 2.96 (dd, H_8, 1 H, J = 4.8, 8.0), 3.52, 3.54 (s, $2CH_3$, 6 H), 3.91 (dd, H_4, 1 H, J = 7.6), 4.23 (q, CH_2, 2 H), 4.36 (dd, H_3, 1 H, J = 6.4), 4.70 (t, H_9, 1 H, J = 7.7), 5.76 (bd, H_{12}, 1 H), 6.78 (d, H_{10}, 1 H), 6.80–7.20 (m, Ph-H, 10 H)
5e	0.85, 0.92 (t, $2CH_3$, 6 H), 1.31 (t, CH_3, 3 H), 2.96 (dd, H_8, 1 H, J = 4.9, 8.4), 3.90 (dd, H_4, 1 H), 3.98 (q, $2CH_2$, 4 H), 4.24 (q, CH_2, 2 H), 4.37 (dd, H_3, 1 H), 4.62 (t, H_9, 1 H, J = 8.8), 5.72 (b d, H_{12}, 1 H), 6.78 (d, H_{10}, 1 H), 6.92–7.18 (m, Ph-H, 10 H)

[a] $CDCl_3$. Abbreviations: d, doublet; s, singlet; m, multiplet; b, broad; q, quartet.

Table III. ^{13}C NMR Spectra[a] of Cage Ketones

compd	chem shift, ppm
5a	9.49, 12.01 (CH_3), 14.47 (CH_3), 43.42 (C-4), 45.23 (C-3), 45.89 (C-8), 48.52, 50.86 (C-1, C-2), 53.85 (C-12), 57.48, 66.97 (C-5, C-7), 62.52 (CH_2), 105.35 (C-9), 153.28 (CO_2), 214.10 (C-6)
5b	8.44, 9.55 (CH_3), 14.47 (CH_3), 16.58, 19.69 (CH_2), 39.90 (C-2), 41.31 (C-3), 45.59 (C-8), 50.04, 53.67 (C-1, C-2), 54.32 (C-12), 60.76, 67.27 (C-5, C-7), 62.52 (CH_2), 105.64 (C-9), 153.28 (CO_2), 214.10 (C-6)
5c	14.47 (CH_3), 14.59, 14.88 (CH_3), 17.52, 18.46, 25.84. 29.12 (CH_2), 40.49 (C-4), 41.84 (C-3), 45.53 (C-8), 50.21, 53.03 (C-1, C-2), 54.32 (C-12), 60.41, 67.21 (C-5, C-7), 62.52 (CH_2), 105.76 (C-9), 153.28 (CO_2), 214.10 (C-6)
5d	14.41 (CH_3), 41.78 (C-4), 43.36 (C-3), 45.70 (C-8), 51.97 (CH_3), 52.44 (C-12), 53.77, 57.83 (C-1, C-2), 62.81 (CH_2), 65.21, 68.03 (C-5, C-7), 102.13 (C-9), 153.22 (CO_2), 166.57, 167.63 (CO_2), 197.58 (C-6)
5e	13.48, 13.71 (CH_3), 14.41 (CH_3), 41.43 (C-4), 43.30 (C-3), 45.47 (C-8), 51.86, 57.54 (C-1, C-2), 52.44 (C-12), 60.29, 60.76 (CH_2), 62.64 (CH_2), 65.10, 67.62 (C-5, C-7), 102.42 (C-9), 153.10 (CO_2), 165.99, 167.11 (CO_2), 197.69 (C-6)

[a] $CDCl_3$.

carbonyl stretching frequency (1800 cm^{-1}) is 50 cm^{-1} higher,[5] and CMR chemical shift of keto carbonyl carbon is 16 ppm lower for **5d** and **5e** than for **5a–c**.

Molecular Structure Determination of 5d. The structure of **5d** was established by X-ray analysis to be the expected [2 + 2] adduct, 1,2-diphenyl-5,7-bis(methoxycarbonyl)-11-ethoxycarbonyl)-11-azapentacyclo[5.5.0.$0^{2,5}$,$0^{3,12}$.$0^{4,8}$]dodeca-9-en-6-one (Figure 1).

Table IV. Final Positional Parameters (×10^4) of Nonhydrogen Atoms with Estimated Standard Deviations in Parentheses

atom	x	y	z
C(1)	7049 (2)	7994 (3)	4623 (4)
C(2)	7947 (2)	7315 (3)	4457 (4)
C(3)	8570 (2)	8042 (3)	3706 (4)
C(4)	7783 (3)	6817 (3)	1896 (4)
C(5)	7365 (2)	6004 (3)	2626 (4)
C(6)	6099 (2)	5713 (3)	2444 (4)
C(7)	6137 (2)	6988 (3)	2810 (4)
C(8)	6701 (2)	6928 (3)	1369 (4)
C(9)	6921 (3)	7988 (3)	1156 (4)
C(10)	7439 (3)	9231 (3)	2364 (4)
N(11)	7901 (2)	9802 (2)	4125 (3)
C(12)	8072 (2)	9025 (3)	4673 (4)
O(13)	5321 (2)	4808 (2)	2194 (3)
C(14)	6562 (2)	8377 (3)	6139 (4)
C(15)	5622 (3)	7463 (3)	6081 (5)
C(16)	5206 (3)	7786 (4)	7508 (5)
C(17)	5706 (3)	9019 (4)	8989 (5)
C(18)	6623 (3)	9932 (4)	9057 (4)
C(19)	7051 (3)	9613 (3)	7643 (4)
C(20)	8465 (3)	7443 (3)	6008 (4)
C(21)	7860 (3)	6620 (3)	6417 (4)
C(22)	8336 (4)	6761 (4)	7887 (5)
C(23)	9406 (4)	7712 (4)	8956 (5)
C(24)	10011 (3)	8526 (4)	8566 (5)
C(25)	9547 (3)	8398 (4)	7091 (4)
C(26)	7714 (3)	4940 (3)	2162 (4)
O(27)	7287 (2)	4134 (3)	2385 (4)
O(28)	8563 (2)	4984 (2)	1439 (3)
C(29)	8950 (4)	3968 (4)	907 (5)
C(30)	5013 (2)	7073 (3)	2546 (4)
O(31)	4114 (2)	6175 (2)	1621 (3)
O(32)	5168 (2)	8295 (2)	3361 (3)
C(33)	4195 (3)	8501 (4)	2906 (6)
C(34)	8254 (2)	11094 (3)	5370 (4)
O(35)	8728 (2)	11650 (2)	6874 (3)
O(36)	8011 (2)	11659 (2)	4679 (3)
C(37)	8482 (4)	13064 (4)	5834 (6)
C(38)	8465 (7)	13523 (5)	4825 (7)

Table VI. Interatomic Distances (Å) with Estimated Standard Deviations in Parentheses

C(1)–C(2)	1.657 (5)	C(14)–C(15)	1.394 (6)
C(1)–C(7)	1.558 (5)	C(14)–C(19)	1.379 (6)
C(1)–C(12)	1.552 (5)	C(15)–C(16)	1.389 (7)
C(1)–C(14)	1.505 (5)	C(16)–C(17)	1.369 (7)
C(2)–C(3)	1.557 (5)	C(17)–C(18)	1.371 (7)
C(2)–C(5)	1.560 (5)	C(18)–C(19)	1.387 (6)
C(2)–C(20)	1.480 (5)	C(20)–C(21)	1.391 (6)
C(3)–C(4)	1.550 (5)	C(20)–C(25)	1.382 (6)
C(3)–C(12)	1.530 (5)	C(21)–C(22)	1.380 (7)
C(4)–C(5)	1.566 (5)	C(22)–C(23)	1.368 (8)
C(4)–C(8)	1.528 (5)	C(23)–C(24)	1.367 (8)
C(5)–C(6)	1.519 (5)	C(24)–C(25)	1.390 (7)
C(5)–C(26)	1.493 (6)	C(26)–O(27)	1.185 (6)
C(6)–C(7)	1.549 (5)	C(26)–O(28)	1.326 (5)
C(6)–O(13)	1.193 (5)	O(28)–C(29)	1.456 (6)
C(7)–C(8)	1.566 (5)	C(30)–O(31)	1.189 (5)
C(7)–C(30)	1.500 (5)	C(30)–O(32)	1.332 (5)
C(8)–C(9)	1.493 (6)	O(32)–C(33)	1.452 (6)
C(9)–C(10)	1.310 (6)	C(34)–O(35)	1.200 (5)
C(10)–N(11)	1.402 (5)	C(34)–O(36)	1.334 (5)
N(11)–C(12)	1.464 (5)	O(36)–C(37)	1.461 (6)
N(11)–C(34)	1.370 (5)	C(37)–C(38)	1.397 (10)

The final atomic coordinates are given in Tables IV and V, and structural parameters in Tables VI and VII.

The two phenyl groups of **5d** are nearly in the face-to-face disposition: twist angles (ϕ_r)[6] of ring planes with regard to the C_1–C_2 bond are −81.4 and 95.5° for C_1-phenyl, and 82.7 and −96.4° for C_2-phenyl ring (Table IX). The nitrogen atom (N_{11})

(5) A reviewer pointed out that the carbonyl absorption by the electron-attracting substituents on α-carbons generally causes a shift to higher frequency by a through-space mechanism. However, our cases can not be interpreted satisfactorily by only this mechanism. In general, IR absorption band of the carbonyl group in the cycloadducts of 2,5-bis(methoxycarbonyl)-3,4-diphenyl-cyclopentadienone and dienophiles exhibited about 20 cm^{-1} higher than the case of 2,5-dimethyl-3,4-diphenylcyclopentadienone (see ref 4b). This difference might be attributed to the through-space interaction.

(6) Hounshell, W. D.; Dougherty, D. A.; Hummel, J. P.; Mislow, K. *J. Am. Chem. Soc.* **1977**, *99*, 1916.

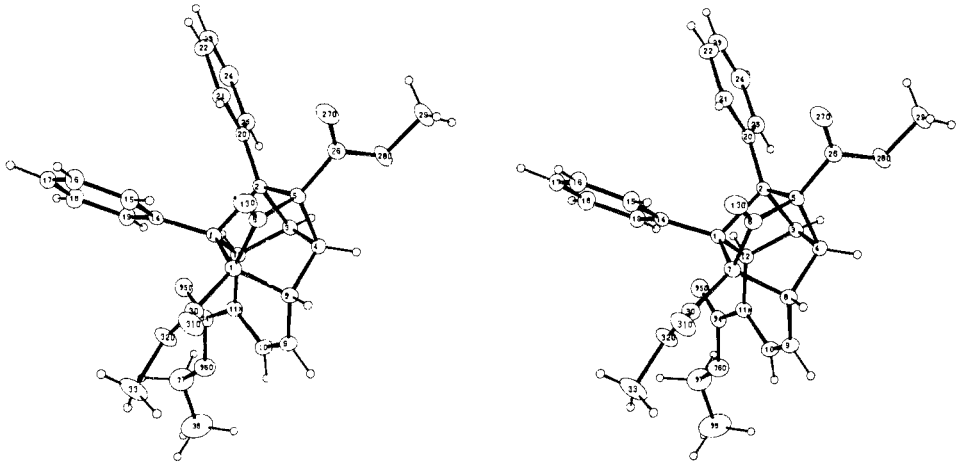

Figure 1. Stereoscopic view by ORTEP of the molecular structure of 1,2-diphenyl-5,7-bis(methoxycarbonyl)-11-(ethoxycarbonyl)-11-azapentacyclo-[5.5.0.0^{2,5}.0^{3,12}.0^{4,8}]dodeca-9-en-6-one (**5d**). The thermal ellipsoids are drawn at 20% probability level, but the hydrogen atom thermal parameters have been arbitrarily reduced for clarity.

Table VII. Interatomic Angles (Deg) with Estimated Standard Deviations in Parentheses

C(2)-C(1)-C(7)	101.6 (3)	C(9)-C(10)-N(11)	124.9 (4)
C(2)-C(1)-C(12)	84.5 (3)	C(10)-N(11)-C(12)	119.9 (3)
C(2)-C(1)-C(14)	117.7 (3)	C(10)-N(11)-C(34)	122.2 (3)
C(7)-C(1)-C(12)	113.3 (3)	C(12)-N(11)-C(34)	117.8 (3)
C(7)-C(1)-C(14)	114.8 (3)	C(1)-C(12)-C(3)	90.2 (3)
C(12)-C(1)-C(14)	119.9 (3)	C(1)-C(12)-N(11)	122.1 (3)
C(1)-C(2)-C(3)	85.5 (3)	C(3)-C(12)-N(11)	122.8 (3)
C(1)-C(2)-C(5)	103.2 (3)	C(1)-C(14)-C(15)	120.2 (3)
C(1)-C(2)-C(20)	117.9 (3)	C(1)-C(14)-C(19)	121.8 (3)
C(3)-C(2)-C(5)	92.6 (3)	C(15)-C(14)-C(19)	118.0 (4)
C(3)-C(2)-C(20)	126.2 (3)	C(14)-C(15)-C(16)	120.8 (4)
C(5)-C(2)-C(20)	123.3 (3)	C(15)-C(16)-C(17)	120.2 (5)
C(2)-C(3)-C(4)	86.6 (3)	C(16)-C(17)-C(18)	119.6 (5)
C(2)-C(3)-C(12)	88.7 (3)	C(17)-C(18)-C(19)	120.5 (5)
C(4)-C(3)-C(12)	115.7 (3)	C(14)-C(19)-C(18)	120.9 (4)
C(3)-C(4)-C(5)	92.6 (3)	C(2)-C(20)-C(21)	120.4 (4)
C(3)-C(4)-C(8)	111.0 (3)	C(2)-C(20)-C(25)	120.6 (4)
C(5)-C(4)-C(8)	103.1 (3)	C(21)-C(20)-C(25)	119.0 (4)
C(2)-C(5)-C(4)	85.9 (3)	C(20)-C(21)-C(22)	120.2 (4)
C(2)-C(5)-C(6)	101.8 (3)	C(21)-C(22)-C(23)	120.4 (5)
C(2)-C(5)-C(26)	120.1 (3)	C(22)-C(23)-C(24)	119.9 (5)
C(4)-C(5)-C(6)	105.8 (3)	C(23)-C(24)-C(25)	120.5 (5)
C(4)-C(5)-C(26)	120.4 (3)	C(20)-C(25)-C(24)	120.0 (4)
C(6)-C(5)-C(26)	117.5 (3)	C(5)-C(26)-O(27)	125.0 (4)
C(5)-C(6)-C(7)	98.8 (3)	C(5)-C(26)-O(28)	111.9 (3)
C(5)-C(6)-O(13)	130.7 (4)	O(27)-C(26)-O(28)	123.1 (4)
C(7)-C(6)-O(13)	130.5 (3)	C(26)-O(28)-C(29)	116.0 (3)
C(1)-C(7)-C(6)	101.1 (3)	C(7)-C(30)-O(31)	125.0 (4)
C(1)-C(7)-C(8)	109.8 (3)	C(7)-C(30)-O(32)	110.9 (3)
C(1)-C(7)-C(30)	119.0 (3)	O(31)-C(30)-O(32)	123.9 (4)
C(6)-C(7)-C(8)	96.6 (3)	C(30)-O(32)-C(33)	116.1 (3)
C(6)-C(7)-C(30)	117.7 (3)	N(11)-C(34)-O(35)	125.1 (4)
C(8)-C(7)-C(30)	110.1 (3)	N(11)-C(34)-O(36)	110.7 (3)
C(4)-C(8)-C(7)	99.7 (3)	O(35)-C(34)-O(36)	124.3 (4)
C(4)-C(8)-C(9)	114.5 (3)	C(34)-O(36)-C(37)	115.6 (4)
C(7)-C(8)-C(9)	118.3 (3)	O(36)-C(37)-C(38)	108.4 (5)
C(8)-C(9)-C(10)	127.6 (4)		

deviates only 0.07 Å from the plane of three neighboring atoms. In fact, C_9, C_{10}, N_{11}, and ester CO_2 atoms are almost in one plane, forming a resonance-stabilized vinylurethane structure in accordance with the IR and UV spectral data (see Experimental Section).

Rather unexpected was the conformation of methoxycarbonyl groups adjacent to 6-keto group. The observed structure involves three carbonyl dipoles aligned in almost the same direction. Such a conformer should be less stable than other conformers having antiparallel carbonyl orientations.[7] This point will be discussed later in this paper.

(7) Allinger, N. L.; Dasen-Micovic, L.; Viskosil, J. F., Jr.; Tribble, M. T. *Tetrahedron*, **1978**, *34*, 3395.

Table XI. Thermolyses of Cage Ketones

compd	R	mp, °C	yield, %	IR ν(C=O), cm^{-1} CHCl$_3$	IR ν(C=O), cm^{-1} Nujol	UV[a] λ_{max}, nm	UV[a] ϵ_{max}
6a	Me	104-107	87	1690	1697	244	20 800
6b	Et	102-104	82	1690	1690	245	27 900
6c	Pr	82-84	91	1690	1710	245	23 900
6d	CO_2Me	96-98	85	1705	1705 (b)	279	19 500
6e	CO_2Et	88-89	89	1700	1700 (b)	282	22 500

[a] Ethanol.

Table XII. ^{1}H NMR[a] Spectra of Tricyclic Dienes

compd	chem shift, δ (J, Hz)
6a	1.20 (b s, CH_3, 3 H), 1.81, 1.92 (s, 2CH_3, 6 H), 2.57 (dd, H_1, 1 H, J = 2.8, 8.0), 3.28 (b s, H_2, 1 H, J = 4.0), 3.59 (b s, H_5, 1 H, J = 3.0), 4.14 (q, CH_2, 2 H), 5.14 (t, H_9, 1 H, J = 9.2), 5.38 (b s, H_6, 1 H), 6.63 (d, H_8, 1 H), 6.72-7.34 (m, Ph-H, 10 H)
6b	0.96-1.26 (m, 2CH_3, 6 H), 1.09 (t, CH_3, 3 H), 1.72-2.58 (m, 2CH_2, 4 H), 2.66 (dd, H_1, 1 H, J = 2.6, 8.4), 3.43 (b s, H_2, 1 H), 3.56 (b s, H_5, 1 H), 4.14 (q, CH_2, 2 H), 5.12 (b s, H_9, 1 H, J = 9.6), 5.34 (b s, H_6, 1 H), 6.60 (d, H_8, 1 H), 6.70-7.27 (m, Ph-H, 10 H)
6c	0.74-2.56 (m, 2$CH_2CH_2CH_3$, 14 H), 0.96 (t, CH_3, 3 H), 2.65 (dd, H_1, 1 H, J = 2.6, 8.0), 3.38 (b s, H_2, 1 H), 3.56 (b s, H_5, 1 H), 4.13 (q, CH_2, 2 H), 5.13 (b s, H_9, 1 H, J = 9.2), 5.32 (b s, H_6, 1 H), 6.62 (d, H_8, 1 H), 6.68-7.32 (m, Ph-H, 10 H)
6d	1.26 (b s, CH_3, 3 H), 3.44, 3.78 (s, 2CH_3, 6 H), 3.50 (dd, H_1, 1 H, J = 3.2, 8.8), 3.60-3.82 (m, H_2, H_5, 2 H), 4.19 (q, CH_2, 2 H), 5.17 (t, H_9, 1 H, J = 10.0), 5.60 (b s, H_6, 1 H), 6.70 (d, H_8, 1 H), 6.78-7.96 (m, Ph-H, 10 H)
6e	0.84 (t, 2CH_3, 6 H), 1.33 (t, CH_3, 3 H), 3.50 (dd, H_1, 1 H, J = 3.2, 8.5), 3.60-3.82 (m, H_2, H_5, 2 H), 3.90 (q, 2CH_2, 4 H), 4.23 (q, CH_2, 2 H), 5.18 (t, H_9, 1 H, J = 9.5), 5.58 (b s, H_6, 1 H), 6.70 (d, H_8, 1 H), 6.76-8.00 (m, Ph-H, 10 H)

[a] $CDCl_3$. See Table II for abbreviations.

The C_1–C_{14} and C_6–C_7 bonds are longer than the corresponding C_2–C_{20} and C_5–C_6 bonds, respectively. The differences might be attributed to the degree of steric congestion around them.

Of the two cyclobutane rings, one ($C_2C_3C_4C_5$) is planar, each atom deviating less than 0.03 Å from the mean plane.[8] The other ring ($C_1C_2C_3C_{12}$) is strongly puckered, C_{12} being displaced 0.63 Å out of the plane defined by the other three atoms. The main planes of these two cyclobutane rings meet at the C_2–C_3 bond with an angle of 74°.

(8) See paragraph at the end of paper regarding supplementary material.

Table XIII. ^{13}C NMR[a] Spectra of Tricyclic Dienes

compd	chem shift, ppm
6a	13.95, 19.98 (CH_3), 14.36 (CH_3), 39.43 (C-1), 44.59 (C-2), 48.75 (C-5), 57.07 (C-6), 61.87 (CH_2), 108.52 (C-9), 153.28 (CO_2)
6b	11.54, 14.00 (CH_3), 14.41 (CH_3), 21.74, 26.43 (CH_2), 37.32 (C-1), 43.83 (C-2), 46.82 (C-5), 57.01 (C-6), 61.87 (CH_2), 109.45 (C-9), 153.28 (CO_2)
6c	14.48, 14.41 (CH_3), 14.41 (CH_3), 20.57, 22.44, 30.70, 35.45 (CH_2), 37.62 (C-1), 43.95 (C-2), 47.23 (C-5), 57.07 (C-6), 61.87 (CH_2), 109.45 (C-9), 153.28 (CO_2)
6d	14.36 (CH_3), 34.34 (C-1), 44.18 (C-2), 45.06 (C-5), 51.15, 51.33 (CH_3), 56.54 (C-6), 62.52 (CH_2), 107.8 (C-9), 152.99 (CO_2), 162.24, 167.51 (CO_2)
6e	13.48, 14.30 (CH_3), 14.30 (CH_3), 34.22 (C-1), 44.18 (C-2), 45.23 (C-5), 56.89 (C-6), 60.06, 60.23 (CH_2), 62.52 (CH_2), 108.05 (C-9), 153.05 (CO_2), 161.95 (CO_2)

[a] $CDCl_3$.

Table XIV. Rate Constants for Decomposition of the Cage Ketones

compd	T, °C	solvent	$10^6 k$(R),[a]	k(R)/k(Me)	E_a, kcal/mol	$\Delta S^{\ddagger}$, eu
1a	162.8	B[b]	7.81			
	172.8	B	20.3	1		
1b	162.8	B	24.7			
	172.8	B	86.4	4.3		
1c	162.8	B	38.5			
	172.8	B	124	6.1		
1d	120.5	ODCD[c]	10.5			
	125.0	ODCD	17.5			
	131.7	ODCD	36.7		34.1	
	133.9	ODCD	52.3			
	139.9	ODCD	76.4			2.6
	162.8	B	862			
	162.8	ODCD	749[g]			
	162.8	B[d]	845			
	162.8	B[e]	804			
	162.8	A[f]	372			
	172.8	B	2060	101		
	172.8	ODCD	1810[g]			
	184.5	ODCD	4850			
1e	162.8	B	602			
	172.8	B	1660	83		

[a] Measured by the ampule technique. The average error is ±3%. [b] Benzene. [c] *o*-dichlorobenzene. [d] Benzene with hydroquinone. [e] Benzene with diphenylamine. [f] Acetonitrile. [g] Extrapolated value.

The most remarkable feature of the molecular structure of **5d** is an exraordinarily long C_1–C_2 bond (1.657 (5) Å).[9] It will be tempting to account for the bond lengthening in terms of combined strains caused by inserting the three-atom bridge ($C_9C_{10}N_{11}$) into the inherently strained homocubane skeleton and repulsion between the facing phenyl groups. However, we reject the mechanical strain interpretation for the reasons discussed below.

Chart I

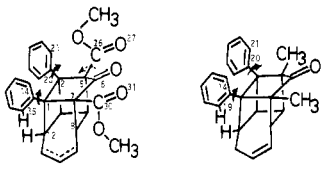

7 8

Kinetics of Decarbonylation. Pyrolyses of cage ketones **5a–e** at 180 °C gave tricyclic trienes **6a–e** in nearly quantitative yields (Table XI).

The product structures are consistent with their NMR spectra (Tables XII and XIII). Kinetic data (Table XIV) were collected by using the ampule technique combined with TLC analysis. The reaction follows the first-order rate law. The rate generally increases with the size of substituent R. Among the various R's examined, alkoxycarbonyls are more effective than *n*-alkyls in increasing the rate. For example, **5d** decarbonylates 100 times faster than **5a**. The rate does not change by the addition of radical trapping agents and is insensitive to the change in solvent polarity. The range of rate change between the slowest solvent acetonitrile and the fastest benzene is only 2.3. These observations indicate concerted bond breaking.[10]

Discussion

Origin of the Long C(Ph)–C(Ph) Bond in 5d. If the unusual length of the C(Ph)–C(Ph) bond of **5d** prevails in the corresponding bonds of **1**, **3** and **5**, the observed propensity of this type of molecules in the decarbonylation reaction must be triggered by these thermally labile bonds.[11] Previous calculations on model structures of **1** *not carrying phenyl groups* indicated that the strain arising from the insertion of three-atom bridge X was not large enough to cause significant elongation of C_1–C_2 bond.[2a,3] In order to take into account the repulsive interaction between the two juxtaposed phenyl rings across the C_1–C_2 bond as well, we carried out potential energy calculations on new models, **7** (three bridge carbon atoms all sp^2 hybridized) and **8**, by using Allinger's MMPI force field[12] (Table XV).

We soon realized that free relaxation of these model structures always led to equilibrium conformations having ϕ_r considerably larger than 90° (Table XV) as the result of twisting of the Ph–C bond in the direction shown in the structure drawing. Hence, calculations were repeated while keeping at 90° by using the DRIVER option.[12d] However, regardless of the final orientation of phenyl groups, the calculated C_1–C_2 bond length of **7** and **8** remains only slightly longer than normal. Thus, we reiterate that the "mechanical" strain cannot be the dominant cause of the observed elongation of C_1–C_2 bond in **5d** and, by implication, may not be the sole driving force in the high thermal reactivities of **5** and related molecules.[2a]

A close look at the calculated structures of **7** and **8** indicates that the "perpendicular" conformation suffers from steric repulsion between H_{12} and H_{19} as the result of the displacement of C_{12} from the planar cyclobutane position by X bridge. The twist of phenyl groups relieves this nonbonded interaction. Thus, the observed crystal conformation of **5d** is probably 5 kcal/mol higher in steric energy than the hypothetical conformation with twisted phenyl groups (compare total steric energies of freely relaxed and constrained **7**, Table XV). If this apparent destabilization of **5d** is

(9) For a comilation of long C–C bonds, see ref 6. More recently reported examples are the following. (a) 1.601 Å: Hazell, A. C.; Weigelt, A. *Acta Crystallogr., Sect. B* **1976**, *B32*, 306. (b) 1.592 Å: Hazell. A. C. *Ibid.* **1976**, *B32*, 2010. (c) 1.606 Å: Hazell, A. C.; Hazell, R. G. *Ibid.* **1977**, *B33*, 360. (d) 1.589 Å: Greenhouse, R.; Borden, W. T.; Hirotsu, K.; Clardy, J. *J. Am. Chem. Soc.* **1977**, *99*, 1664. (e) 1.638 Å: Lüttke, W.; Druck, U. *Angew. Chem.* **1979**, *91*, 434. (f) 1.661 Å: Knowx, J. R.; Raston, C. L.; White, A. H. *Aust. J. Chem.* **1979**, *32*, 553. (g) 1.644 Å: Ferguson, J.; Man, W.-H.; Whimp, P. O. *J. Am. Chem. Soc.* **1979**, *101*, 2370. (h) 1.609 Å: Khaikim, L. S.; Belyakov, A. V.; Koptev, G. S.; Golubinskii, A. V.; Kirin, V. N.; Koz'min, A. S.; Vilkov, L. V.; Yarovoi, S. S. *J. Mol. Struct.* **1978**, *60*, 55. (i) 1.667 Å: Hisatome, M.; Kawaziri, Y.; Yamakawa, K.; Iitaka, Y. *Tetrahedron Lett.* **1979**, 1777. (j) 1.851 and 1.783 Å: Bianchi, R.; Pilati, T.; Simonetta, M. *Acta Crystallogr., Sect. A* **1978**, *B34*, 2157. (k) 1.827 and 1.771 Å: Bianchi, R.; Morosi, G.; Mugnoli, A.; Simonetta, M. *Ibid.* **1973**, *B29*, 1196. (l) 1.72 Å: Barrow, M. J.; Mius, O. S. *J. Chem. Soc. A* **1971**, 1982.

(10) Rubio, M.; Hernandez, A. G.; Daudey, J. P.; Cetina, R. R.; Diaz, A. *J. Org. Chem.* **1980**, *45*, 150.

(11) Other examples of fast thermal reactions starting at the long bond: (a) Isomura, K.; Hirose, Y.; Shuyama, H.; Abe, S.; Ayabe, G.; Taniguchi, H. *Heterocycles* **1978**, *9*, 1207. (b) Berridge, J. C.; Bryce-Smith, D.; Gilbert, A.; Cantrell, T. S. *J. Chem. Soc., Chem. Commun.* **1975**, 611. (c) Jones, P. G.; Kirby, A. J. *Ibid.* **1979**, 288. (d) Beckhans, H-D.; McCullough, K. J.; Fritz, H.; Rüchardt, C.; Kitschke, B.; Lindner, H. J.; Dougherty, D. A.; Mislow, K. *Chem. Ber.* **1980**, *113*, 1867 and preceding papers of this series.

(12) Wertz, D. H.; Allinger, N. L. *Tetrahedron* **1974**, *30*, 1597. Allinger, N. L.; Sprague, J. T. *J. Am. Chem. Soc.* **1973**, *95*, 3893. (c) Allinger, N. L.; Sprague, J. T.; Liljefors, T. *Ibid.* **1974**, *96*, 5100. (d) Allinger, N. L.; Yuh, Y. H. *QCPE* **1979**, *11*, 318.

Table XV. MMPI Calculations of Diphenylpentacyclic Ketones 7 and 8

	phenyl orientation[a]	dihedral angles, deg				C_1–C_2 length, Å	steric energy, kcal/mol	
		$C_1C_2C_{20}C_{21}$[b]	$C_2C_1C_{14}C_{19}$[b]	$C_6C_5C_{26}O_{27}$	$C_6C_7C_{30}O_{31}$		C=O[c]	total
7	forced ⊥	88.57	99.79	−36.13	−8.37	1.5722	15.61	120.00
	free relax	98.60	127.05	7.27	−7.16	1.5653	15.24	114.85
7a	free relax	99.72	129.69	6.03	168.21	1.5657	13.33	113.29
7b	free relax	98.83	129.78	176.71	−6.95	1.5646	13.54	112.53
7c	free relax	98.72	129.11	175.27	166.87	1.5656	11.56	111.47
8	forced ⊥	89.39	91.28			1.5809	3.03	105.49
	free relax	93.10	124.43			1.5688	3.55	85.24

[a] In forced perpendicular orientation, phenyl groups were fixed perpendicular relative to the C_1–C_2 bond, as in the crystal structure of **5d**, using the dihedral angle driver option of the program.[12d] In freely relaxed calculations, these dihedral angle constraints were removed to reach energy minimum. [b] ϕ_r, twist angle of phenyl plane relative to the C_1–C_2 bond. [c] The sum of steric energy terms around carbonyl group. For the concept of local strain, see ref 4.

Chart II

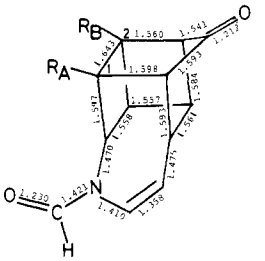

9a, R = C_6H_5
9b, R = H
9c, R = CH_3

not caused by the crystal-packing force, some electronic effect that compensates for the extra strain must be involved. The observed elongation of the C_1–C_2 bond and the perpendicular orientation of the phenyl groups indicate a possibility of the "through-bond" interaction between π systems.[13]

Semiempirical SCF MO calculations on MNDO approximation[14] combined with the geometrical optimization by the Fletcher–Powell method[15] of another model of **5d**, namely **9a**, reproduced the observed structural parameters of **5d** quite well, including the C_1–C_2 bond length (see calculated bond lengths in the structure drawing of **9a**).[16] Replacement of the two phenyl groups with H (**9b**) and repeated MNDO geometry optimization resulted in contraction of the C_1–C_2 bond to 1.5847 Å, in reasonable agreement with the MMPI results of **7** and **8**. Furthermore, Mulliken's overlap population[17,18] at the C(Ph)–C(Ph) bond of **9a** increased significantly when the phenyl groups were replaced with methyl (**9c**) and the geometry was reoptimized while keeping the $C(CH_3)$–$C(CH_3)$ bond at the previous length (Table XVI). For C–Ph bonds of **9a**, the lengths are quite short and the overlap populations quite high.

Replacement of phenyl groups with methyl (**9c**) led to increased lengths and lowered populations of the corresponding bonds (C–CH_3). These are the indications of the migration of electron population from the C_1–C_2 bond to the C–Ph bond by the "through-bond" coupling in **9a**.

Table XVI. Characteristics of C(R)–C(R) and C–R Bonds of Model Structures 9–12

		R = C_6H_5 (a)			R = CH_3 (c)	
		length, Å		MNDO overlap pop.	MNDO length, Å	MNDO overlap pop.
		MMPI	MNDO			
9	C(R)–C(R)	1.5653	1.6435	0.9280	(1.6435)[a]	0.9530
	C–R A	1.5080	1.5164	1.2633	1.5101	1.2188
	B	1.5003	1.4990	1.2871	1.5021	1.2341
10	C(R)–C(R)	1.5553	1.6118	0.9469	(1.6118)[a]	0.9807
	C–R	1.4907	1.4924	1.3261	1.5004	1.2433
11	C(R)–C(R)	1.5826	1.5961	0.9069	(1.5961)[a]	1.0115
	C–R	1.5230	1.5092	1.3000	1.5147	1.2067
12	C(R)–C(R)	1.5420	1.5531	1.0947	(1.5531)[a]	1.2210
	C–R	1.5151	1.5165	1.2545	1.5287	1.2367

[a] The length fixed at the value obtained with phenyl substituents.

Chart III

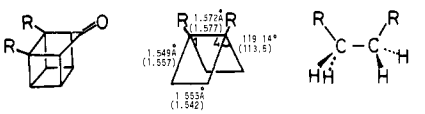

10 11 12

a, R = C_6H_5; b, R = H; c, R = CH_3

Mislow's studies on the "through-bond" interactions in *p,p'*-dibenzene and related molecules[13c] suggest that such interactions take place even if a C–C bond is connected to only one π system in the right geometry. Compounds **9a** and **5d** are certainly eligible in this respect for this interaction. However, according to Mislow's estimation,[13c] a bond correctly surrounded by two π systems is lengthened only by 0.012 Å or the expected C_1–C_2 bond length of **5d** will be at the most 1.60 Å on this basis. Even among the known examples of very long C–C bonds,[9,13c] those exceeding 1.64 Å are a rarity. Why did such a pronounced bond elongation occur in **9a** and **5d**? Clearly, high prestraining of the C_1–C_2 bond must have worked to transmit the π coupling more effectively than the less strained σ bond does. We discuss below the validity of this hypothesis.

Since the calculated molecular orbitals of **9a** are too complex for further analysis due to complete lack of symmetry, we first turned to a simpler model **10** (C_s point group). The same responses as in **9** were observed with this model in the C(R)–C(R) and C–R bonds regarding their lengths and overlap populations when R was changed from Ph to CH_3. Nevertheless, the MO's of **10a** proved still too complex to analyze visually. Furthermore, contrary to some other strained cage ketones which also undergo thermal decarbonylation,[10] **10a** (and also **9a**) showed negative Mulliken overlap populations between C_1, C_2 and carbonyl atoms: the carbonyl group should not be directly responsible for the bond elongation. Thus, the model structure for our present purpose can be simpler than **10**.[19] We finally settled upon unknown

(13) (a) Hoffmann, R. *Acc. Chem. Res.* **1977**, *4*, 1. (b) Dougherty, D. A.; Hounshell, W. D.; Schlegel, H. B.; Bell, R. A.; Mislow, K. *Tetrahedron Lett.* **1976**, 3479. (c) Dougherty, D. A.; Schlegel, H. B.; Mislow, K. *Tetrahedron* **1978**, *34*, 1441. (d) Hemmersbach, P.; Klessinger, M.; Bruckmann, P. J. *Am. Chem. Soc.* **1978**, *100*, 6344. (e) Schoeller, W. W. *J. Chem. Soc., Perkin Trans 2* **1979**, 366.

(14) Dewar, M. J. S.; Thiel, W. *J. Am. Chem. Soc.* **1977**, *99*, 4899, 4907.

(15) Thiel, W. *QCPE* **1979**, *11*, 353. The QCPE version of the MNDO program was expanded to accommodate 100 atoms, 250 basis orbitals, and 200 eigenvalues, and a new option for computing Mulliken's overlap population was added. We thank Dr. W. Thiel for valuable instructions.

(16) Two ϕ_r values were kept at 90°.

(17) Mulliken, R. S. *J. Chem Phys.* **1955**, *23*, 1833.

(18) See however: (a) Collins, J. B.; Streitwieser, A., Jr. *J. Compt. Chem.* **1980**, *1*, 81. (b) Streitwieser, A., Jr.; Collins, J. B.; McKelvey, J. M.; Grier, D.; Sender, J.; Toczko, A. G. *Proc. Natl. Acad. Sci. U.S.A* **1976**, *76*, 2499. (c) Collins, J. B.; Streitwieser, A., Jr.; McKelvey, J. M. *Comput. Chem.* **1979**, *3*, 79.

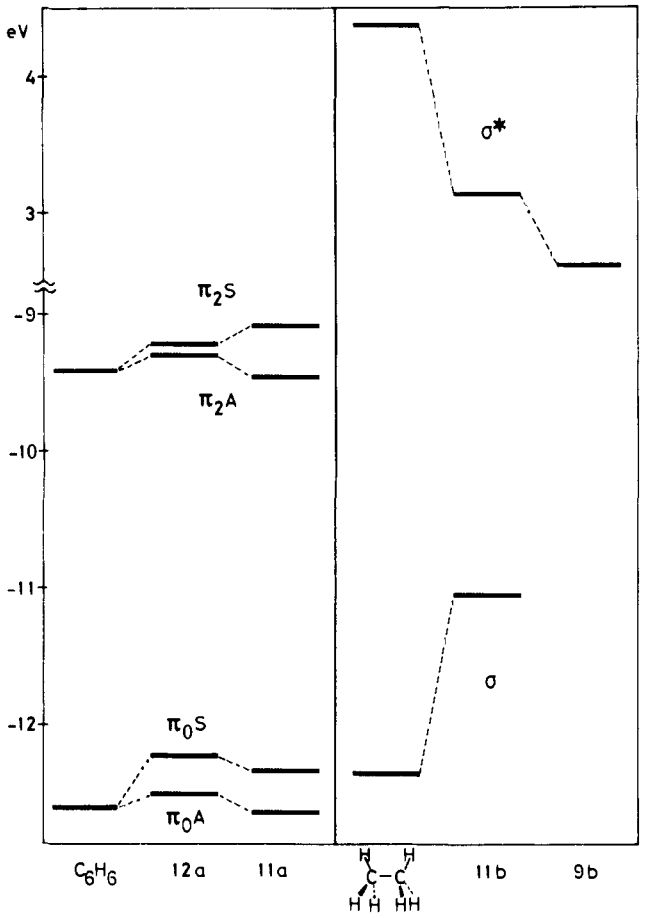

Figure 2. Level diagram of molecular orbitals of model molecules pertinent to illustrate interactions between phenyl groups through unstrained and strained C–C bonds. π_0 and π_2 refer to the molecular orbital dominated by the benzene-type bonding π orbitals with zero and two nodes. S and A refer to symmetric and antisymmetric property of the MO with regard to a plane bisecting the C–C bond vicinally substituted by phenyl groups. Energy is in electronvolt unit.

1,4-diphenylbicyclo[2.2.0]hexane with the phenyl rings oriented perpendicular to C_1–C_4 bond (**11a**). The MNDO-optimized geometry of parent hydrocarbon (**11b**) agrees well with the electron diffraction values[20,21] (figures given in the structure drawing correspond to the bond lengths and C–C–C angles of **11b** with experimental values in parentheses). Upon introduction of the phenyl groups (**11a**) the MNDO C_1–C_4 bond length increased to approximately 1.6 Å. The C(R)–C(R) and C–R bonds behave similarly as those of **9** and **10** by changing the phenyl groups to methyl groups (**11c**, Table XVI). Therefore, there certainly exist the "through-bond" interactions in **11a**. This molecule has an ideal symmetry (C_{2v}) in that the local phenyl group π orbitals retain the feature of familiar benzene orbitals, which facilitates the analysis described below.

1,2-Diphenylethane in the eclipsed, perpendicular conformation (**12a**) was also chosen as the simplest possible model of **5d** having essentially an unstrained C–C central bond. The molecule has been well studied,[22] but the possibility of "through-bond" interaction in this conformation has never been suggested. Our combined force field and MNDO calculations on **12a** and **12c** suggest a small "through-bond" interaction in terms of the bond length and overlap population criteria (Table XVI). Figure 2 illustrates calculated levels of interesting molecular orbitals of our models and other relevant molecules. Among the three bonding π-type local orbitals of the phenyl group, one of the degenerate orbitals ($\pi_{2'}$) has a node at the point of attachment to the rest of molecule and should exert no influence on the "through-bond" interactions. Therefore, we consider only those MO's which contain the other two nodes (π_2) and zero-node (π_0) local benzene-type MO's for the diphenyl-substituted models. For saturated models, MO's predominantly σ and σ^* characters of the C_1–C_2 bond are entered in the figure. The MNDO levels of the corresponding MO's of benzene as well as the CC σ and σ^* orbitals of eclipsed ethane (Figure 2) will give an idea on the depths of levels before perturbation. The symmetry notations, S and A, refer to the symmetry regarding a plane passing through the center of C–C bond in question.

Chart IV

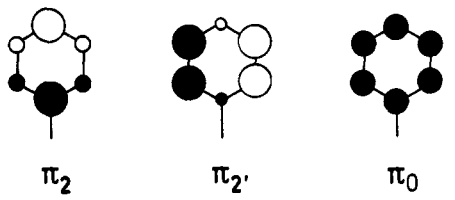

Chart V

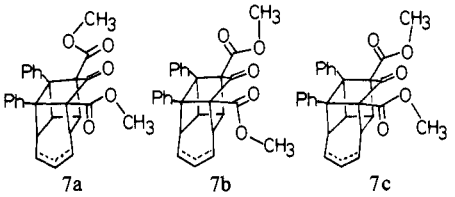

In *syn*-1,2-diphenylethane (**12a**), the π_2S orbital that results from antibonding mixing of the C_1C_2 σ orbital with $\pi_2 + \pi_2$ combination of phenyl local orbitals is higher in energy than the π_2A orbital that involves bonding contribution from C_1C_2 σ^* level into the π_2–π_2 combination.[23] The same is true with π_0S and π_0A. Such reversal of orbital level (otherwise π_s should be lower than π_A) is the most characteristic feature of the "through-bond" interaction.[13,23] Nevertheless, the extent of level reversal is so small that its effect on bond length in **12a** is almost unperceived (Table XVI).

In 1,4-diphenylbicyclo[2.2.0]hexane (**11a**), the separation between π_2S and π_2A is much larger than that of **12a**, apparently as the result of better orbital mixing involving lower σ^* and higher σ "original" orbitals (see **12b**) with π orbitals compared to the case for **11**. The separation among π_0-type orbitals of **11a** was of the same magnitude as that of **12a**. Concerning **9**, we note here that one of the very low-lying antibonding MO's of **9b**, the unperturbed model of **9a**, is dominated by C_1C_2 σ^* character. This suggests a strong possibility of high antibonding character in the C_1C_2 bond of **9a**, leading to bond elongation as large as 0.06 Å. It is very probable that the same interpretation applies to **5d** as well.

Conformation of Methoxycarbonyl Groups in Crystalline 5d. According to Allinger,[7] a conformation of 3,3-dimethyl-2,4-pentanedione having two carbonyl dipoles in a syn-parallel fashion is 2–8 kcal/mol less stable than the others having anti-parallel carbonyl orientations. In this respect, the observed conformation

(19) In this respect, 1,2-diphenylcubane is interesting since this molecule should have one of the most strained σ bonds. However, MNDO is known to give rather unsatisfactory results for extremely strained molecules such as bicyclo[1.1.0]butane.[14] MNDO geometry optimization of cubane itself gave C–C bond length of 1.5713 Å and heat of formation of 99.055 kcal/mol, both very different from the observed values (1.552 Å[19a] and 148.70 kcal/mol[19b]). (a) Fleisher, E. B. *J. Am. Chem. Soc.* **1964**, *86*, 3889. (b) Cox, J. D.; Pilcher, G. "Thermochemistry of Organic and Organometallic compounds"; Academic Press: New York, 1970.

(20) Andersen, B.; Srinivasan, R. *Acta Chem. Scand.* **1972**, *26*, 3468.

(21) The MNDO-optimized geometry has near C_{2v} symmetry whereas the observed structure has C_2 symmetry (due to puckered cyclobutane rings). However, this defect is not crucial for the present purpose. The agreement between MNDO-calculated and observed central C–C bond lengths is excellent.

(22) (a) Cruickshank, D. W. J. *Acta Crystallogr.* **1949**, *2*, 65. (b) Ivanov, P.; Pojarlieff, I.; Tyutyukov, N. *Tetrahedron Lett.* **1976**, 775. (c) Ivanov, P.; Pojarlieff, I. *J. Mol. Struct.* **1977**, *38*, 259.

(23) The bonding and antibonding combinations of two phenyl group π orbitals, before interacting with C–C bond, are supposed to have nearly identical energy levels. For the illustrations of the "through-bond" coupling principle, see: ref 13a and Jorgenson, W. L.; Salem, L. "The Organic Chemist's Book of Orbitals"; Academic Press: New York, 1973; p 27.

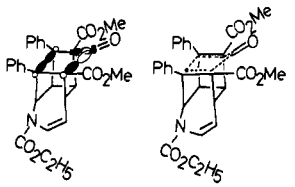

Figure 3. Schematic illustration of proposed decarbonylation transition state of **5d**.

of **5d** should be the least stable compared to other conformers resulting from rotations of C_5–C_{26} and C_7–C_{30} bonds. Molecular mechanics calculations of model structures **7a**, **7b**, and **7c** confirm that the anti,anti conformer **7c** is the most stable (Table XV). We have checked that no energy minimum conformation arises during the rotation of ester groups in **7** and **7a–c** by performing bond-drive calculations.[24,25]

Decarbonylation Reaction. The importance of perpendicular phenyl conformation at C_1 and C_2 as observed in **5d** to effect the thermal ring opening giving **6** is well demonstrated. It is likely that the C_1–C_2 bonds of the other isomers (**5a–c** and **5e**) are also long and thermally labile, playing a key role in the decarbonylation reaction. The present series of **5** allows us to probe into the effects of changing the substituents R at C_5 and C_7 on the reaction rate. The alkyl series, methyl, ethyl, and *n*-propyl, increases the rate in this order by small but significant magnitudes (Table XIV). Since the frontier orbital theory[26] normally predicts lowered reactivities for ethyl and *n*-propyl than for metyl derivaties,[27] F-strain effects appear to be operating here. Namely, a small increase in the congestion around the leaving carbonyl groups will lead to a slight decrease in the activation energy.

Much more pronounced rate enhancement (up to 100-fold) was obtained by replacing alkyl with alkoxycarbonyl groups (Table XIV). Both the frontier orbital interactions and steric factors seem responsible. Let us first examine steric contribution. Steric congestion around the carbonyl group in the ground state of **5d,e** has already been indicated by the abnormal infrared and ^{13}C NMR frequencies (vide supra), and this should lead to enhanced rates due to the F strain. The extent of F strain can be best measured by calculating local strain[3] around the carbonyl group by molecular mechanics. For the model structures **7** and **7a–c**, the calculated congestion proved to be 8–12 kcal/mol higher than that of **8**, the model of **5a** (see the column under the heading of steric energy, C=O, Table XV). The major contributor to this large difference is the electrostatic repulsion between polar bonds in close proximities. Nonbonded repulsion plays only a minor role (12–16% of the total local strain), the largest contribution coming from the short distance between H_8 and the carbonyl carbon C_6 (calculated 2.39 Å for **7**, **7a–c**; observed 2.41 Å for **5d**). This close approach is caused by the outward displacement of C_8 due to the vinylurethane bridge, like that in C_{12}.[28]

The fontier orbital theoretical view on the rate enhancement in **5d,e** is that the interactions of the LUMO of the ketonic bridged C_5–C_6 and C_6–C_7 bonds with the HOMO of the elongated C_1–C_2 bond are assisted by the electronegative alkoxycarbonyl group (Figure 3).

Finally, we must record our reservation on the concertedness of this reaction. Baldwin[29] has reported that thermal decarbonylation of dicyclopentadien-1,8-dione occurs with a $\Delta S^{\ddagger}$ of 9.8 ± 2.3 eu, and this value lies close to the rotational entropy of carbon monoxide, suggestive of a decarbonylation transition state in which both bonds to the carbon monoxide moiety have been broken. In our study, the entropy of activation is significantly lower than the Baldwin value (Table XIV) and the possibility of only one of the bonds between bridgehead carbon and the keto group being broken in the transition state cannot be denied.

Conclusion

Reflections on the structure and mechanism of the novel decarbonylation ring-opening reaction of **5** to **6** by means of X-ray analysis, kinetics, and various available theoretical approaches uncovered several novel features of this reaction. First, the hitherto mysterious role of aryl substituents at the C_1–C_2 bond can now be explained: the bond must be thermally labile and this lability is achieved by straining the strained σ bond further by the "through-bond" π coupling. Second, the remarkable rate enhancement by the introduction of the alkoxycarbonyl groups adjacent to the keto group appears well explained in terms of steric and frontier orbital theories.

These results can be utilized to the further exploitation of the reversible reaction between **2** and **3**. The elongation of the prestrained σ bond by simply introducing phenyl substituents appears to be a general phenomenon, and more detailed studies on this subject will be reported shortly.

Experimental Section

The melting points were measured with a Yanagimoto micromelting point apparatus and are uncorrected. The UV spectra were determined with a Hitachi EPS-3T spectrometer. The NMR spectra were taken with a JEOL PS-100 spectrometer with tetramethylsilane as an internal standard. The IR spectra were taken with a JASCO IRA-1 infrared spectrophotometer. Mass spectra were obtained with a JEOL JMS-01SG double-focusing spectrometer operating at an ionization potential of 75 eV. The solid samples were ionized by electron bombardment after sublimation directly into the electron beam at 150–200 °C. Thin-layer chromatographic analyses were performed with a Iatron TH-10 TLC analyzer with a flame ionization detector.

Cyclopentadienone. 2,5-Diethyl, 2,5-dipropyl, and 2,5-bis(ethoxycarbonyl) derivatives of 3,4-diphenylcyclopentadienones were prepared by a general method.[30]

2,5-Diethyl-3,4-diphenylcyclopentadienone: mp 100–103 °C; yield 45%; IR (Nujol) 1710 cm^{-1} (CO). Anal. ($C_{21}H_{20}O$) C, H.

2,5-Dipropyl-3,4-diphenylcyclopentadienone: mp 74–76 °C; yield 57%; IR (Nujol) 1710 cm^{-1} (CO). Anal. ($C_{23}H_{24}O$) C, H.

2,5-Bis(ethoxycarbonyl)-3,4-diphenylcyclopentadienone: mp 119–120 °C; yield 52%; IR (Nujol) 1730 (CO), 1710 cm^{-1} (COOEt). Anal. ($C_{23}H_{20}O_5$) C, H.

Cycloaddition Reaction of 2,5-Disubstituted-3,4-diphenylcyclopentadienones with *N*-(Ethoxycarbonyl)azepine. The procedure is similar to that described in the previous paper.[31] The known compounds (**4a,d**) were identified by comparison of spectral data with those of authentic samples.[31] For new compounds **4b,c,e**, yields and physical properties are summarized as follows.

4b: mp 148–150 °C; yield 38%; IR (Nujol) 1690, 1710 cm^{-1}; NMR ($CDCl_3$) δ 0.8–1.4 (m, 11 H), 2.36 (q, 2 H), 2.90 (t, 1 H), 4.16 (m, 2 H), 5.05 (t, 1 H), 5.18 (b d, 1 H), 5.63 (t, 1 H), 6.23 (t, 1 H), 6.68 (d, 1 H), 7.2–7.4 (m, 10 H). Anal. ($C_{30}H_{31}NO_3$) C, H, N.

4c: mp 98–100 °C; yield 76%; IR (Nujol) 1695, 1710 cm^{-1}; NMR ($CDCl_3$) δ 0.61 (b t, 3 H), 0.86 (t, 3 H), 1.04–1.72 (m, 9 H), 2.2–2.4 (m, 2 H), 2.86 (t, 1 H), 4.14 (m, 2 H), 5.04 (t, 1 H), 5.16 (b d, 1 H), 5.61 (t, 1 H), 6.22 (t, 1 H), 6.69 (d, 1 H), 7.1–7.4 (m, 10 H). Anal. ($C_{32}H_{35}NO_3$) C, H, N.

(24) Because of the large amount of CPU time necessary to perform bond-drive calculations with MMPI system, MMI[12d] was used and the phenyl ring was treated "mechanically" by using new stretch force constant (8.0667 mdyn/Å) and equilibrium distance (1.3937 Å) for aromatic carbon atoms (type 2-2).[12b]

(25) In contrast, 3,3-dimethyl-2,4-pentanedione has energy minimum conformations involving two perpedicular carbonyl planes.[7]

(26) Levitt, L. S.; Levitt, B. M.; Parkanyi, C. *Tetrahedron* **1972** *28*, 3369.

(27) Inagaki, S.; Fujimoto, H.; Fukui, K. *J. Am. Chem. Soc.* **1976** *98*, 4693.

(28) Cursory bond drive calculations of **7** and **7a–c** around C_5–C_{26} and C_7–C_{30} bonds mentioned above revealed rather low barriers of rotation. For example, the barriers of going from **7** to **7b** is 8.3 kcal/mol. Namely, the four conformers of **5d** (and **5e** as well) which arise during the rotation of the ester group and correspond to **7**, **7a**, **7b**, and **7c** should rapidly equilibrate under the reaction conditions. Even for the presumed dominant conformer **7c**, the steric congestion around the carbonyl group is considerably higher than that of **8** (Table XV). Another interesting observation made during the drive calculations is that the rotation of ester plane does not seriously affect the twist angle of the adjacent phenyl group. The maximum change of ϕ_r during the C_5–C_{26} bond drive of **7** was 10°, showing the twist. Namely, the twist movements of phenyl and ester planes are hardly correlated (cf. Ōsawa, E. *J. Am. Chem. Soc.* **1979** *101*, 5523). This excludes a possible role of the bulky groups at C_5 and C_7 acting as a buttressing body to cause perpendicular ϕ_r, thus promoting the elongation of the C_1–C_2 bond.

(29) Baldwin, J. E. *Can. J. Chem.* **1966**, *44*, 2051.

(30) Ashida, T. "SIGMA, The Universal Crystallographic Computing System (I)"; The Crystallographic Society of Japan, 1967; pp 43–44.

(31) Germain, G.; Main, P.; Woolfson, M. M. *Acta Crystallogr., Sect. A* **1971**, *27A*, 368.

4e: mp 198–201 °C, yield 74%; IR (Nujol) 1700, 1740 cm^{-1}; NMR ($CDCl_3$) δ 0.72 (t, 3 H), 1.16 (t, 3 H), 3.22 (t, 1 H), 4.24 (q, 6 H), 5.2–5.7 (m, 3 H), 6.40 (t, 1 H), 6.70 (d, 1 H), 7.2–7.6 (m, 10 H).

Syntheses of 1,2-Diphenyl-5,7-disubstituted-11-(ethoxycarbonyl)-11-azapentacyclo[5.0.0^{2,5}.0^{3,12}.0^{4,8}]dodeca-9-en-6-ones (5a-e). General Procedure. A solution of **4a–e** (1.95 mmol) in benzene (20 mL) was irradiated through a Pyrex jacket with a 100-W high-pressure mercury lamp under nitrogen at room temperature for 20 min. After removal of the solvent, the solid residue was recrystallized from EtOH–acetone. The results are summarized in Tables I–III.

Thermolyses of Cage Ketones (Syntheses of 3,10-Disubstituted-4,11-diphenyl-7-(ethoxycarbonyl)-7-azatricyclo[4.3.2.0^{2,5}]undeca-3,9,10-trienes (6a–e)). A benzene solution (5 mL) of **5a** (0.98 mmol) was heated at 180 °C for 3 h in a sealed tube. After removal of the solvent, the oily residue was purified on a silica gel column eluting with hexane–ethyl acetate to afford **6a**. The product was recrystallized from n-hexane–benzene. Thermolyses of **5b–e** in a similar manner gave **6b–e**. The results are listed in Tables XI–XIII.

Kinetics. Thermolyses rate studies of **5a–e** were conducted at about 0.7 mmol/L in the given solvents (see Table XIV) in sealed tubes which were thermostated with flowing oil at constant temperatures. Portions were taken at various times. In *o*-dichlorobenzene solution, the rates were determined spectrometrically by following the increase of the absorption at 320 nm to the methyl cinnamate chromophore. On the other hand, in the other solvents the rates were followed by a thin-layer chromatographic analyzer. The kinetic data are summarized in Table XIV.

X-ray Crystallography. Crystal Data. $C_{30}H_{27}NO_7$ (**5d**), M_r = 513.6: triclinic, a = 12.835 (5) Å, b = 13.514 (5) Å, c = 9.523 (4) Å, α = 122.19 (3)°, β = 93.44 (3)°, γ = 108.33 (3)°, V = 1266 (1) Å^3, D(measd) = 1.318 g cm^{-3}, D(calcd) = 1.345 g cm^{-3}, Z = 2, F(000) = 512, MoKα radiation, λ = 0.7107 Å. Crystals from ethanol by slow evaporation at room temperature. Crystals of the compound are colorless parallelepipeds. The density was measured by flotation in aqueous potassium iodide solution. The cell constants were stablished from a least-squares procedure using the values of the Bragg angles of 15 reflections measured on a Syntex P$\bar{1}$ four-circle diffractometer with Mo Kα radiation.

The space group $P\bar{1}$ (No. 2) was selected from the number of molecules per unit cell (Z = 2) and was later confirmed in the course of the structure refinement. Intensity data were collected on a Syntex P$\bar{1}$ automated diffractometer with Mo Kα radiation monochromated by a graphite crystal using the θ–2θ scan technique to a limit of 2θ = 55°. The variable scan rate from 24.0 to 4.0 min^{-1} was adopted. Three reflections were monitored after every measurement of 97 reflections. Of the 3989 independent reflections, 2842 were treated as observed ($I > 2.3\sigma(I)$). The intensities were corrected for Lorentz and polarization effects, but no correction was applied for absorption.

Structure Solution and Refinement. An overall temperature factor of 3.71 Å^2 was obtained from a Wilson plot and used to calculate normalized structure factors.[30] The structure was solved by the direct method using the MULTAN[31] series of programs. An E map calculated with 475 signed E's ($|E| > 1.5$), which gave the figure of merit (ABS FOM) of 1.1858, revealed the positions of all the expected nonhydrogen atoms. Six cycles of isotropic refinement and 9 cycles of anisotropic refinement led to a R index of 0.0828. At this stage, all the hydrogens were located from a difference electron density map. After adding the hydrogens but with keeping their thermal parameters fixed, we obtained a final R of 0.047. Both thermal and positional parameters of the five hydrogens attached to the ethyl group of the urethane moiety were fixed for their markedly anisotropic vibrations. In final refinements, the following weights were used for the observed reflections: $w = 1.0$ for $F_o < 40.0$, $w = 1600/F_o^2$ for $F_o \geq 40.0$. The atomic scattering factors were taken from the "International Tables for X-ray Crystallography" (1974). All the calculations were performed on the FACOM M-200 computer in the Computer Center of Kyushu University with the Universal Crystallographic Computation Program System (UNICS II).[32]

Acknowledgment. Calculations have been performed at the Computer Centers of Kyushu University, Hokkaido University, and the Institute for Molecular Sciences. H. Dantsuji, A. Tsurumoto, and Y. Onuki provided technical assistance during earlier stages of this work.

Supplementary Material Available: Final thermal parameters of nonhydrogen atoms (Table XVII), final atomic parameters of hydrogen atoms (Table V), least-squares best planes (Table VIII), important torsion angles (Table IX), intermolecular contacts less than 3.50 Å involving nonhydrogen atoms (Table X), a view of the packing of molecules in the crystals (Figure 4), and a listing of observed and calculated structure amplitudes (16 pages). Ordering information is given on any current masthead page.

(32) Sakurai, T.; Iwasaki, J.; Watanabe, Y.; Kobayashi, K.; Bando, Y.; Nakamichi, Y. *Rikagaku Kenkyusho Hookoku* **1974**, *50*, 75.